

RESEARCH

Open Access



# Neurologic symptoms as a hallmark of glymphatic alteration in recovered patients with COVID-19

Minhoe Kim<sup>1†</sup>, Kyung Hoon Lee<sup>2†</sup>, Ji Su Ko<sup>2</sup>, Myung Sub Kim<sup>2</sup>, Kyu Sung Choi<sup>3</sup>, Jiwon Seo<sup>4\*</sup> and Minchul Kim<sup>2\*</sup>

## Abstract

**Background** The glymphatic system is a glial-based perivascular network that facilitates the clearance of metabolic waste from the brain. Dysfunction of the glymphatic system, along with neurological symptoms such as cognitive deficits and olfactory dysfunction, has been reported in patients with coronavirus disease (COVID-19). However, the link between these neurological symptoms and alterations in the glymphatic system remains unclear. In this study, we aimed to evaluate magnetic resonance imaging (MRI)-based measures of the glymphatic system in patients recovered from COVID-19 with and without neurological symptoms.

**Methods** This study included 89 patients who recovered from respiratory infections, of whom 71 had confirmed COVID-19 (20 experienced anosmia and 41 had cognitive symptoms). Three MRI-based measures were quantified and compared: the dilated perivascular spaces (dPVS), free water (FW) fraction, and diffusion tensor image analysis along the perivascular spaces (DTI-ALPS). A partial correlation network was used to assess the relationships between COVID-19 infection, neurological symptoms, and glymphatic measures.

**Results** COVID-19 patients with anosmia had increased FW in the left orbitofrontal area compared to those without anosmia (mean difference: 0.01,  $p=0.48$ ), while patients with cognitive symptoms showed decreased left-sided DTI-ALPS (mean difference: 0.06,  $p=0.40$ ). Neurological symptoms mediate the relationship between COVID-19 and glymphatic system measures.

**Conclusions** Our findings imply that neurological symptoms accompanied by COVID-19 are linked to distinct alterations in the glymphatic system, suggesting a potential association between neuroinvasion and neuroinflammatory processes related to COVID-19.

<sup>†</sup>Minhoe Kim and Kyung Hoon Lee contributed equally to this work.

\*Correspondence:

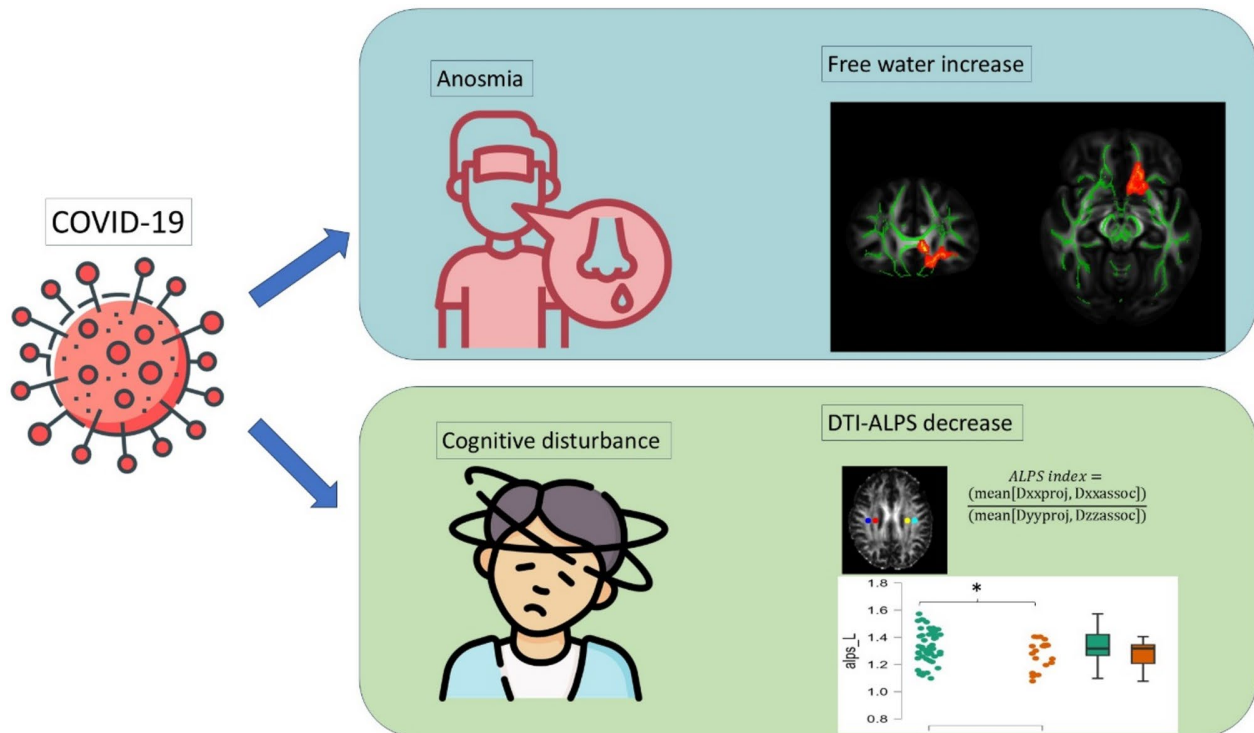
Jiwon Seo  
mangiinyu@gmail.com  
Minchul Kim  
minchulusa@gmail.com

Full list of author information is available at the end of the article



© The Author(s) 2025. **Open Access** This article is licensed under a Creative Commons Attribution-NonCommercial-NoDerivatives 4.0 International License, which permits any non-commercial use, sharing, distribution and reproduction in any medium or format, as long as you give appropriate credit to the original author(s) and the source, provide a link to the Creative Commons licence, and indicate if you modified the licensed material. You do not have permission under this licence to share adapted material derived from this article or parts of it. The images or other third party material in this article are included in the article's Creative Commons licence, unless indicated otherwise in a credit line to the material. If material is not included in the article's Creative Commons licence and your intended use is not permitted by statutory regulation or exceeds the permitted use, you will need to obtain permission directly from the copyright holder. To view a copy of this licence, visit <http://creativecommons.org/licenses/by-nc-nd/4.0/>.

## Graphic Abstract



## Key points

- Previous literature indicates alterations in the glymphatic system following COVID-19 infection.
- We explore the differences between post-COVID patients with and without neurologic symptoms using MRI-based measures of the glymphatic system.
- We demonstrate that post-COVID patients with neurologic symptoms exhibit altered MRI-based measures of the glymphatic system.
- These findings suggest that glymphatic alterations associated with COVID-19 may involve direct neuroinvasion and neuroinflammatory processes.

**Keywords** Glymphatic alteration, COVID-19, DTI-ALPS, Anosmia

## Background

Although coronavirus disease (COVID-19) predominantly affects the respiratory system, its long-term consequences include numerous neurological and neurocognitive symptoms [1]. For example, olfactory dysfunction has gained widespread attention as post-COVID-19 anosmia cases have surged since the start of the pandemic [2]. Therefore, the World Health Organization (WHO) included several neurological symptoms such as anosmia and cognitive dysfunction as common symptoms in its definition of post-COVID-condition [3].

The glial-lymphatic or glymphatic system was recently identified as the waste-clearance mechanism in the brain. According to the glymphatic hypothesis [4], cerebrospinal fluid (CSF) from the subarachnoid space enters the brain's interstitial space via the periarterial pathways, where it mixes with the interstitial fluid (ISF)

and accumulates waste solutes. These waste products are subsequently removed from the brain through the perivenous efflux pathway (Fig. 1). Several promising noninvasive MRI-based techniques have recently been developed for indirectly assessing glymphatic activity, including dilated MRI-visible perivascular spaces (dPVS) in the basal ganglia (BG) [5], the fractional volume of free water (FW) in the brain parenchyma (i.e., brain ISF) from a bitensor diffusion tensor imaging (DTI) model [6], and the diffusion along perivascular spaces (DTI-ALPS) index [7–9] (Fig. 1, bottom row).

Severe acute respiratory syndrome coronavirus 2 (SARS-CoV-2) enters the central nervous system (CNS) via two routes: through the hematogenous respiratory pathways or direct neuroinvasion through olfactory receptors [10]. When the virus enters the brain via the olfactory system, it may trigger anosmia and the

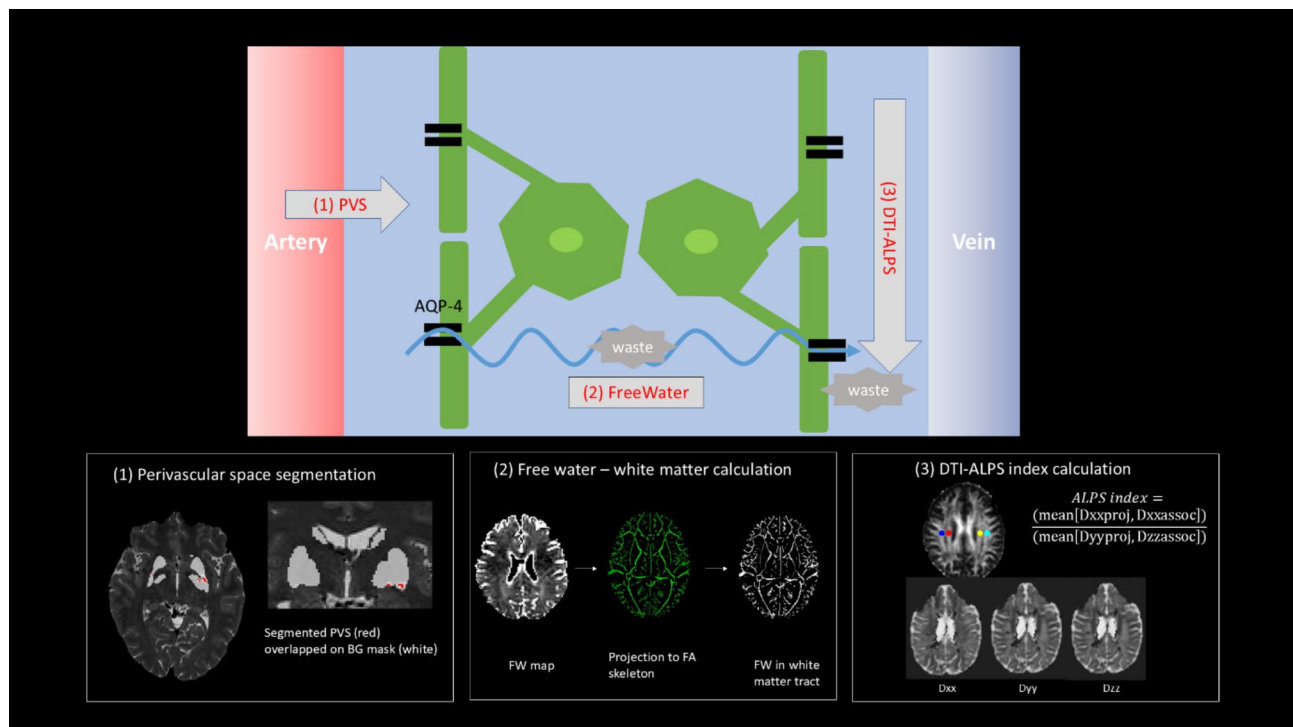


**Fig. 1** Schematic of the glymphatic system (upper row) and MRI-based noninvasive methods (Bottom row). Briefly, from arteries, cerebrospinal fluid (CSF) crosses the perivascular space entering the interstitium through the AQP-4 channel and moving toward perivenous spaces (zigzag arrow). Although formal validation studies are still lacking, we hypothesized that PVS may serve as a proxy for periarterial flow; deterioration in the exchange of CSF and interstitial fluid would increase the extracellular fractional volume of free water (FW); DTI-ALPS measures the diffusivity capacity of the perivenous space surrounding the deep medullary vein at the lateral ventricle body level, enabling the assessment of the CSF outflow channel within this system. Abbreviation: PVS, perivascular space; AQP-4, aquaporin-4; DTI-ALPS, Diffusivity Along the Perivascular Spaces

activation of cerebral mast cells and microglia, resulting in the secretion of proinflammatory molecules, and causing brain inflammation and brain fog [11, 12]. The symptoms of brain fog are associated with various causative factors including cognitive decline, disrupted sleep patterns, and nutritional and mental health deficiencies [13]. Multiple studies have detected glymphatic system dysfunctions in COVID-19 patients using MRI-based assessments, especially among individuals experiencing cognitive decline, sleep disturbances, and neurological symptoms; Wu et al. found asymmetrical DTI-ALPS impairment in mild COVID-19 cases, particularly in older patients and those with cognitive issues [10], while Zhou et al. demonstrated reduced CSF [18 F]-radiolabelled phenoxyanilide (18 F-FEPPA) clearance in post-COVID patients with neurological symptoms [14]. Additionally, Del Brutto et al. found a link between poor sleep quality post-COVID and dPVS, and Langan et al. observed increased dPVS, indicating neuroinflammation [15]. However, studies on anosmia and neurological symptoms as independent risk factors for glymphatic alterations caused by COVID-19 are lacking. This highlights a research gap as systemic inflammation and neuroinvasion by SARS-CoV-2 can alter the glymphatic system [16]. As neurological syndrome may start from

olfactory neuron damage [10], determining whether systemic inflammation or neuroinvasion is responsible for glymphatic alteration would enhance our understanding of the long-term neurological consequences of COVID-19.

In this study, we evaluated whether anosmia or persistent cognitive symptoms could serve as potential markers of glymphatic alterations in adults who recovered from COVID-19, using dPVS, FW, and DTI-ALPS.

## Materials and methods

### Participants

We used the publicly available dataset available at the OpenNeuro repository (<https://openneuro.org/datasets/ds005364/versions/1.0.0>), which included patients recruited in Santiago, Chile during the pandemic (February 2020 to May 2023). Detailed descriptions can be found by Kausel et al. [17]. The dataset comprised 89 adult patients who had mild to moderate respiratory infections, and with available DTI images. Using PCR, 71 were confirmed to have a respiratory infection caused by SARS-CoV-2; of them, 20 experienced anosmia and 41 had persistent cognitive symptoms, including memory and attention deficits. The sample size was additionally determined through power analysis using G\*Power

software based on the effect size reported in a similar study [10, 18]. This study reported a medium effect size of Cohen's  $d = 0.66$ , which corresponds to Cohen's  $f = 0.33$  for the analysis of variance (ANOVA). Using this effect size, a power level of 0.80, and an alpha level of 0.05, the calculation indicated that 74 participants were required to achieve sufficient statistical power. Our study included 71 participants, which closely approximates the calculated requirements.

All participants provided informed consent, and the Ethics Committee of Clínica Alemana, Universidad del Desarrollo, approved all experimental procedures. The consent process and all experimental methods adhered to Chilean national laws, institutional policies, and the Declaration of Helsinki, and this study has the necessary ethical permissions to share the data publicly under a Creative Commons CC0 license (<https://docs.openneuro.org/faq.html>).

#### MRI data acquisition

All participants underwent multiple MRI scans on a 3 Tesla Siemens Skyra scanner (Siemens AG, Erlangen, Germany), including: (1) Sagittal 3D MPRAGE T1-weighted imaging with repetition time (TR)/echo time (TE) = 2530/2.19 ms, inversion time (TI) = 1100 ms, flip angle = 7°, and voxel size =  $1 \times 1 \times 1$  mm<sup>3</sup>; (2) Sagittal 3D T2-weighted imaging with TR/TE = 3200/412 ms, flip angle = 120°, echo train length (ETL) = 258, and voxel size =  $1 \times 1 \times 1$  mm<sup>3</sup>; (3) Sagittal 3D fluid-attenuated inversion recovery (FLAIR) imaging with TR/TE = 5000/388 ms, TI = 1800 ms, ETL = 251, flip angle = 120°, slice thickness = 1 mm, and voxel size =  $1 \times 1 \times 1$  mm<sup>3</sup>; and (4) Axial 3D echo planar imaging (EPI) diffusion imaging with TR/TE = 8600/95 ms, flip angle = 90°, voxel size =  $2 \times 2 \times 2$  mm<sup>3</sup>, and diffusion gradients in 30 non-collinear directions with two b factors ( $b_1 = 0$  and  $b_2 = 1000$  s/mm<sup>2</sup>) across three repetitions. We applied a series of quality controls available in DSI Studio (<http://dsi-studio.labsolver.org>), including: (1) calculating the mean Pearson correlation coefficient of “neighboring” diffusion-weighted images, (2) identifying slice-wise signal dropout for each slice in each diffusion-weighted image, and (3) checking the b-table orientation using the fiber coherence index [19].

#### PVS segmentation

Potential dPVS voxels were detected in T2-weighted images using 3D Frangi filtering implemented through the Python library “skimage” [20]. This method evaluates vessel-like structures based on the eigenvalues of the Hessian matrix and is effective for identifying dPVS in medical imaging research [15, 21]. The 3D Frangi filter was applied to T2-weighted images, followed by thresholding to extract potential dPVS voxels. A threshold

value of 0.25 was chosen for the PVS probability map to generate individual PVS masks, based on the developer's recommendation and visual assessment using various threshold levels (<https://github.com/hufsaim/pvsseg/>). The processed images occasionally included false positives outside the brain, with probable suboptimal PVS segmentation in the deep white matter regions. To address this, a basal ganglia (BG) mask derived from FSL FIRST segmentation was applied to reduce errors [5, 22] (Fig. 1, bottom row (1)). (Fig. 1, bottom row (1)). Finally, the resulting PVS masks were reviewed manually to ensure their quality.

#### FW calculation and voxelwise statistical analysis

We used an approach similar to that mentioned in our previous article [23]. In brief, The DTI images were subject to denoising algorithm and Gibbs unringing using MRtrix3 command line “dwisenoise” and “mrdegibbs,” and eddy current correction was done with FSL “eddy.” FW-corrected DTI maps were calculated using an in-house MATLAB script, fitting a 2-compartment model at each voxel [23–25]. The FW map represents the relative fraction of FW in each voxel, ranging from 0 to 1. A more detailed methodology for this analysis is provided in Supplementary Material. Subsequently, voxel-wise statistical analysis of the diffusion data was conducted using tract-based spatial statistics (TBSS) [26]. Initially, the fractional anisotropy (FA) data from all subjects were aligned to the  $1 \times 1 \times 1$  mm<sup>3</sup> FMRIB58\_FA standard space atlas via nonlinear registration. Subsequently, a mean FA image was generated from the aligned FA images and thinned to form a skeletonized mean FA image representing the central axes of all tracts common to all subjects. The mean FA skeleton was thresholded to  $FA \geq 0.2$ , which is the default value, and each subject's aligned FA data were projected onto the skeleton. Finally, we acquired the mean of the FW index of each participant's white matter skeleton using the ‘tbss\_non\_FA’ command [9] (Fig. 1, bottom row (2)).

Voxel-wise statistical analyses of the FW index maps were subsequently performed on voxels within the white matter skeleton. We employed the ‘randomise’ tool from the FSL program suite to compare COVID-19 patients with anosmia to those without, incorporating the time elapsed between COVID-19 diagnosis and MRI as a covariate. Permutation-based testing (5,000 permutations) and statistical inference were performed with multiple comparisons corrected using threshold-free cluster enhancement (TFCE) [27].

#### ALPS index calculation

The DTI-ALPS index was calculated using an automated method available at <https://github.com/gbarisano/alps> [28]. Each subject's FA map was co-registered to the

JHU-ICBMFA template, and regions of interest (ROIs) were automatically defined as 5 mm diameter spheres within the bilateral superior corona radiata (SCR) and superior longitudinal fasciculus (SLF) (Fig. 1, bottom row). Diffusivity values (Dxx, Dyy, Dzz) from these ROIs were extracted to compute the ALPS index using the following formula:  $\text{mean}(D_{xproj}, D_{xassoc})/\text{mean}(D_{yproj}, D_{zassoc})$ . A lower DTI-ALPS index indicates impaired glymphatic function.

**Statistical analysis**

Statistical analyses were performed using the JASP software [29]. Demographic variables were compared using the chi-square test for categorical data and independent sample t-test for continuous data. Continuous variables are reported as means with standard deviations. Statistical significance was set at  $p < 0.05$ . To evaluate glymphatic alterations, we performed analysis of covariances (ANCOVAs) with MRI-based glymphatic measures (dPVS, FW, and ALPS index) as dependent variables, the time (in months) between COVID-19 diagnosis and MRI as covariates, and group classification (COVID-19 patients with vs. without neurological symptoms, such as anosmia and cognitive issues) as fixed factors. Furthermore, we utilized graphical least absolute shrinkage and selection operator (LASSO) network analysis to explore the relationships among multiple variables, including dPVS, FW, ALPS index, and COVID-19 symptoms [30]. The detailed methodology for this analysis is provided in Supplementary Material.

**Result**

**dPVS**

Demographic and clinical data of the study participants are summarized in Table 1. Two ANCOVAs were performed to test for mean differences in dPVS volume between COVID-19 patients with or without neurological symptoms after controlling for number of months

between COVID-19 diagnosis and MRI. The ANCOVA results indicated no group difference for both anosmia and cognitive symptoms (anosmia,  $F = 0.788, p = 0.378$ ; cognitive symptoms,  $F = 2.451, p = 0.122$ ).

**FW index**

Two ANCOVAs were conducted to test for mean differences between COVID-19 patients with or without neurological symptoms on the FW index after controlling for months between COVID-19 diagnosis and MRI. ANCOVA results indicated a significant group difference between COVID-19 patients with and without anosmia ( $F = 4.066, p = 0.048$ ; Fig. 2(A)). Descriptive statistics indicated that COVID-19 patients with anosmia had higher FW indices than those without anosmia (mean = 0.069 and 0.060, respectively).

The TBSS results revealed a significant area of difference according to anosmia, demonstrating an increased FW (Fig. 3). The main tract involved in the affected areas was the left orbitofrontal area, which encompasses the uncinate fasciculus, inferior fronto-occipital fasciculus, anterior thalamic radiation, and forceps minor.

**DTI-ALPS index**

Two ANCOVAs were conducted to test for mean differences between COVID-19 patients with or without neurological symptoms on the DTI-ALPS index after controlling for months between COVID-19 diagnosis and MRI. ANCOVA results indicated a significant group difference between COVID-19 patients with and without cognitive symptoms ( $F = 4.369, p = 0.040$ , Fig. 2(B)) in the left DTI-ALPS index. Descriptive statistics indicated that COVID-19 patients with cognitive symptoms had a lower left DTI-ALPS index than those without symptoms (mean = 1.334 and 1.278, respectively).

**Table 1** Clinical characteristics of the 71 COVID-19 population

| Cognitive symptoms                               | w/ Cognitive symptoms (n = 29) | w/o Cognitive symptoms (n = 42) | P-value |
|--|--------------------------------|---------------------------------|---------|
| Age (years)                                      | 42.89 ± 11.14                  | 41.61 ± 12.91                   | 0.667   |
| Gender (Male: Female)                            | 17:12                          | 20:22                           | 0.362   |
| Time between COVID-19 diagnosis and MRI (months) | 8.69 ± 4.12                    | 9.95 ± 5.22                     | 0.280   |
| Hospitalization required                         | 12                             | 27                              | 0.939   |
| Anosmia  | w/ Anosmia (n = 51)            | w/o Anosmia (n = 20)            | P-value |
| Age (years)                                      | 41.70 ± 11.14                  | 43.25 ± 13.97                   | 0.634   |
| Gender (Male: Female)                            | 24:27                          | 13:7                            | 0.173   |
| Time between COVID-19 diagnosis and MRI (months) | 9.66 ± 5.13                    | 8.85 ± 3.93                     | 0.524   |
| Hospitalization required                         | 20                             | 9                               | 0.656   |

w/: with; w/o: without

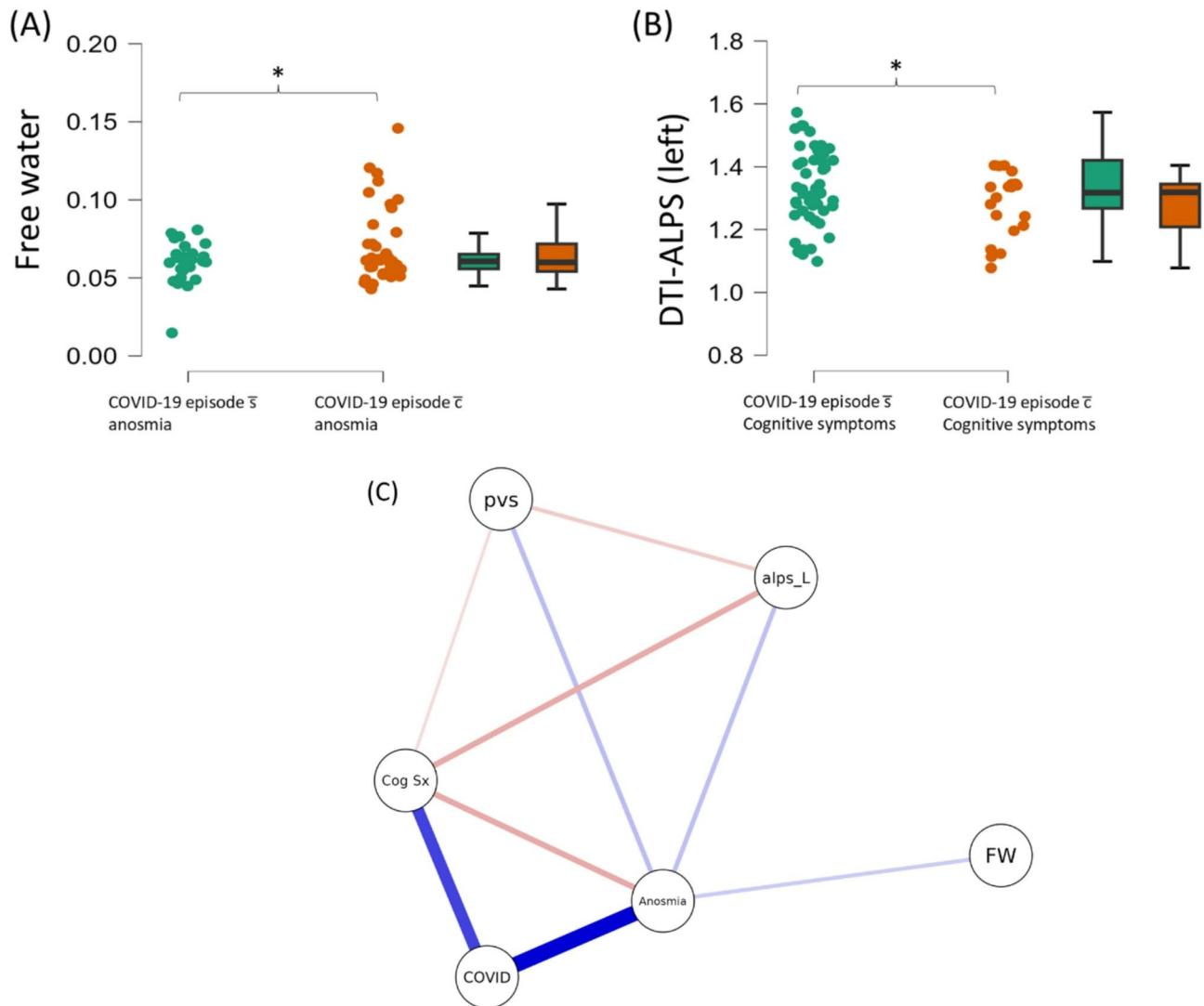


**Fig. 2** Between-group differences in MRI-based measures of the glymphatic system. Panel **(A)** shows the free water increase in COVID-19 with anosmia, while panel **(B)** shows the left side diffusion along the perivascular space (DTI-ALPS) index decrease in COVID-19 with cognitive symptoms than those without. Panel **(C)** shows the network of the COVID-19 infection (COVID), cognitive symptoms (Cog Sx), Anosmia, and MRI-based measures the glymphatic system. Note that COVID is linked to glymphatic system measures via Cog Sx and anosmia. Blue lines represent positive associations, and red lines represent negative associations. Abbreviation:  $\bar{s}$ : without,  $\bar{c}$ : with, pvs: perivascular space, alps\_L: left Diffusivity Along the Perivascular Spaces, FW: extracellular fractional volume of free water. \*  $p < 0.05$

**Network analysis**

The regularized partial correlation network is shown in Fig. 2(C). Several notable features emerged from the analysis. First, a history of COVID was associated with anosmia and cognitive symptoms, but not directly linked to various measures of the glymphatic system. Second, the FW index was solely related to anosmia, suggesting a possible independent relationship with other measures.

**Discussion**

In this study, we aimed to understand how neurological symptoms associated with COVID-19 are linked to changes in the glymphatic system. We used MRI-based

measures to examine the glymphatic system in recovered COVID-19 patients with neurological symptoms and compared these results with those in post-COVID patients without impairments (Fig. 1). We identified two altered MRI-based measures of the glymphatic system in patients with neurological symptoms. The FW index increased in COVID-19 patients with anosmia compared to those without anosmia (Fig. 2A), whereas the left DTI-ALPS index decreased in patients with cognitive symptoms (Fig. 2B). Furthermore, network analysis showed that COVID-19 was indirectly linked to glymphatic system measures through anosmia and cognitive symptoms (Fig. 2C). Our results imply that neurological symptoms

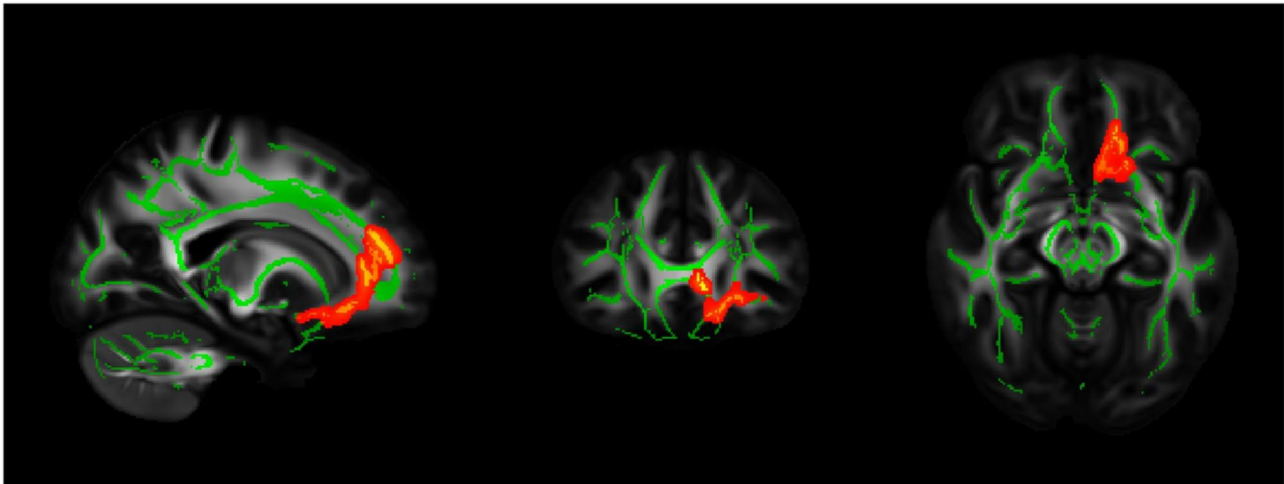


**Fig. 3** TBSS result. Red-yellow voxels represent regions in which free water was increased significantly in COVID-19 with anosmia relative to those without. The recognized tracts encompass left uncinate fasciculus, inferior fronto-occipital fasciculus, anterior thalamic radiation, and forceps minor

reported in COVID-19 patients may serve as an indicator of glymphatic system alterations.

Taken together, our results suggest that neuroinvasion and neuroinflammation by SARS-CoV-2, rather than systemic inflammation, alter the glymphatic system. Anosmia and cognitive disturbances observed in COVID-19 patients likely result from neuroinvasion and subsequent neuroinflammatory processes [31, 32]. Specifically, the COVID-19 virus has been shown to infiltrate the CNS via angiotensin-converting enzyme 2 (ACE 2) widely expressed in the brain as a functional receptor. In contrast, the olfactory epithelium and bulb lead to inflammation in regions such as the orbitofrontal cortex [32]. Meanwhile, the glymphatic system plays a crucial role in eliminating potentially neurotoxic waste products, including  $\beta$ -amyloid, and is particularly significant for neurodegenerative diseases such as Alzheimer's disease [33]. Our results suggest that neurological symptoms are a risk factor for long-term neurological deterioration following COVID-19. Given the constraints on medical resources and the need to prioritize high-risk populations, our findings suggest that recovered COVID-19 patients with a history of neurological symptoms should receive increased attention. Previous reports investigating the implications of neurological symptoms of COVID-19 and brain involvement also support nontrivial symptom-specific brain alterations. Kausel et al. discovered that patients who presented with anosmia exhibited more impulsive behavior, and that anosmia correlated with decreased functional activity during decision-making tasks [17], while hospitalization itself did not alter DTI-ALPS index [34].

From a pathophysiological perspective, we observed an interesting pattern in which FW increased with anosmia in the left orbitofrontal lobe (Fig. 3). Following

COVID-19, anosmia results from infected support cells in the olfactory epithelium, leading to olfactory neuronal damage and reduced olfactory bulb volume [17]. The orbitofrontal areas contain the secondary and tertiary olfactory cortices, which play a crucial role in the conscious perception and evaluation of odor and taste [35–37]. Research indicates that the orbitofrontal lobe receives direct projections from primary olfactory regions such as the piriform cortex and is involved in the integration of olfactory information with other sensory modalities [36]. A potential pathway for the spread of SARS-CoV-2 from the nose to the brain includes olfactory circuits and CSF near the olfactory epithelium, which aligns with the identified regions in our study [38]. Similarly, Hosp et al. discovered an increase in the FW/CSF fraction in the post-COVID-condition group compared to unimpaired post-COVID patients [1]. Taken together, the pattern of FW increase implies a direct relationship between olfactory invasion and glymphatic alterations following COVID-19.

Our study leaves several questions unanswered. First, we did not find any relationship between dPVS and neurological symptoms. One hypothesis is that a decrease in DTI-ALPS may precede an increase in BG-PVS volume, as suggested in a recent study [5]. This time-lagged association supports the idea that decreased DTI-ALPS levels could be an early contributing mechanism for later enlargement of BG-PVS; however, a follow-up confirmatory study is required. In addition, the PVS volumetry in our study was limited to the BG. Although we excluded false positives, the noninclusion of PVS volumetry from other regions may have underestimated the association between PVS volumes and symptoms. Another notable finding was the leftward laterality of glymphatic alteration. We speculate that functional lateralization may be a

clue, e.g. the left orbitofrontal cortex has been associated with emotional olfactory tasks [39], since unilateral DTI-ALPS decrease is often linked with functional lateralization [40, 41].

This study had several limitations. First, although MRI-based measures of the glymphatic system have been considered a proxy for glymphatic function in previous studies [5], they can only approximate glymphatic function. In addition, follow-up studies using advanced MRI techniques for neurodegenerative biomarkers, including quantitative susceptibility mapping and arterial spin labeling-based blood-brain barrier imaging, could reveal potential influences on neurodegeneration [42–45]. Second, our study did not directly confirm the presence of SARS-CoV-2 in the brain, which could have been demonstrated by the detection of viral RNA in the CSF of infected patients [31]. Third, our sample size was relatively small. Although we conducted a power analysis, the subgroup analyses (e.g., anosmia vs. non-anosmia) might still have reduced power owing to the smaller group sizes. Finally, due to the cross-sectional design of our study, we could not establish a causal link between neurological symptoms and glymphatic system alterations.

## Conclusion

MRI-based glymphatic analysis in recovered COVID-19 patients revealed key findings. Patients with anosmia showed a higher FW index, especially in the left orbitofrontal area, linking olfactory dysfunction to altered interstitial fluid volume. Those with cognitive symptoms exhibited a lower left DTI-ALPS index, suggesting impaired glymphatic function related to perivascular diffusivity. Network analysis indicated these glymphatic changes are mediated by anosmia and cognitive symptoms rather than the direct effects of COVID-19. These findings highlight distinct glymphatic alterations associated with neurological symptoms after COVID-19 infection.

## Abbreviations

|                       |   |
|-----------------------|---|
| COVID-19              | Coronavirus Disease   |
| MRI                   | Magnetic Resonance Imaging                                    |
| dPVS                  | dilated Perivascular Space                                    |
| FW                    | Free Water  |
| DTI-ALPS              | Diffusion Tensor Image Analysis along The Perivascular Spaces |
| WHO                   | World Health Organization                                     |
| CSF                   | Cerebrospinal fluid, ISF: Interstitial Fluid                  |
| SARS-CoV-2            | Severe Acute Respiratory Syndrome coronavirus 2               |
| CNS                   | Central Nervous System  |
| <sup>18</sup> F-FEPPA | [ <sup>18</sup> F]-Radiolabelled Phenoxyanilide               |
| ANOVA                 | Analysis of Variance  |
| ANCOVA                | Analysis of Covariance  |
| TE                    | Repetition time   |
| TE                    | echo Time   |
| FLAIR                 | Fluid-Attenuated Inversion Recovery                           |
| EPI                   | Echo Planar Imaging   |
| ETL                   | Echo Train Length   |
| BG                    | Basal Ganglia   |
| TBSS                  | Tract-Based Spatial Statistics                                |

|       |                                    |
|-------|------------------------------------|
| FA    | Fractional Anisotropy              |
| TFCE  | Threshold-Free Cluster Enhancement |
| SCR   | Superior Corona Radiate            |
| ROIs  | Regions Of Interest                |
| SLF   | Superior Longitudinal Fasciculus   |
| ACE 2 | Angiotensin-Converting Enzyme 2    |

## Supplementary Information

The online version contains supplementary material available at <https://doi.org/10.1186/s12883-025-04198-1>.

Supplementary Material 1

## Author contributions

Minhoe Kim: Conceptualization, Software, Investigation, Writing, Funding acquisition. Kyung Hoon Lee: Investigation, Writing. Ji Su Ko: Conceptualization, Investigation, Writing. Myung Sub Kim: Investigation, Writing. Kyu Sung Choi: Investigation, Writing. Jiwon Seo: Conceptualization, Investigation, Writing. Minchul Kim: Conceptualization, Software, Investigation, Writing, Funding acquisition, Visualization.

## Funding

This research was supported by the KBSMC- SKKU Future Clinical Convergence Academic Research Program, Kangbuk Samsung Hospital & Sungkyunkwan University, 2024.

## Data availability

The raw data and analysis results can be found at <https://osf.io/6kz2b/>.

## Declarations

### Ethics approval and consent to participate

All participants gave their informed consent, and the Ethics Committee of Clínica Alemana—Universidad del Desarrollo approved all experimental procedures. The consent process and all experimental methods adhered to Chilean national laws, institutional policies, and the Declaration of Helsinki, and have any necessary ethics permissions to share the data publicly under a Creative Commons CC0 license (<https://docs.openneuro.org/faq.html>).

### Consent for publication

Not applicable.

### Competing interests

The authors declare no competing interests.

### Author details

- <sup>1</sup>Department of Electrical and Information Engineering, Seoul National University of Science and Technology, Seoul, Korea
- <sup>2</sup>Department of Radiology, Kangbuk Samsung Hospital, Sungkyunkwan University School of Medicine, 29 Saemunan-ro, Jongno-gu, Seoul 03181, Republic of Korea
- <sup>3</sup>Department of Radiology, Seoul National University College of Medicine, Seoul, Korea
- <sup>4</sup>Department of Radiology, Research Institute and Hospital of National Cancer Center, 323 Ilsan-ro, Ilsandong-gu, Goyang-si, Gyeonggi-do 10408, Republic of Korea

Received: 16 December 2024 / Accepted: 16 April 2025

Published online: 28 April 2025

## References

- Hosp JA, Reiser M, Dressing A, Götz V, Kellner E, Mast H, Arndt S, Waller CF, Wagner D, Rieg S. Cerebral microstructural alterations in Post-COVID-conditions are related to cognitive impairment, olfactory dysfunction and fatigue. *Nat Commun*. 2024;15(1):4256.

2. Yildirim D, Kandemirli SG, Sanli DET, Akinci O, Altundag A. A comparative olfactory MRI, DTI and fMRI study of COVID-19 related anosmia and post viral olfactory dysfunction. *Acad Radiol*. 2022;29(1):31–41.
3. Organization WH. A clinical case definition of post COVID-19 condition by a Delphi consensus, 6 October 2021. In: World Health Organization; 2021.
4. Xie L, Kang H, Xu Q, Chen MJ, Liao Y, Thiyagarajan M, O'Donnell J, Christensen DJ, Nicholson C, Iliff JJ. Sleep drives metabolite clearance from the adult brain. *Science*. 2013;342(6156):373–7.
5. Li H, Jacob MA, Cai M, Kessels RP, Norris DG, Duering M, De Leeuw F-E, Tuladhar AM. Perivascular spaces, diffusivity along perivascular spaces, and free water in cerebral small vessel disease. *Neurology*. 2024;102(9):e209306.
6. Pasternak O, Sochen N, Gur Y, Intrator N, Assaf Y. Free water elimination and mapping from diffusion MRI. *Magn Reson Medicine: Official J Int Soc Magn Reson Med*. 2009;62(3):717–30.
7. Taoka T, Masutani Y, Kawai H, Nakane T, Matsuoka K, Yasuno F, Kishimoto T, Naganawa S. Evaluation of glymphatic system activity with the diffusion MR technique: diffusion tensor image analysis along the perivascular space (DTI-ALPS) in Alzheimer's disease cases. *Japanese J Radiol*. 2017;35:172–8.
8. Kamagata K, Andica C, Takabayashi K, Saito Y, Taoka T, Nozaki H, Kikuta J, Fujita S, Hagiwara A, Kamiya K. Association of MRI indices of glymphatic system with amyloid deposition and cognition in mild cognitive impairment and Alzheimer disease. *Neurology*. 2022;99(24):e2648–60.
9. Andica C, Kamagata K, Takabayashi K, Kikuta J, Kaga H, Someya Y, Tamura Y, Kawamori R, Watada H, Taoka T. Neuroimaging findings related to glymphatic system alterations in older adults with metabolic syndrome. *Neurobiol Dis*. 2023;177:105990.
10. Wu L, Zhang Z, Liang X, Wang Y, Cao Y, Li M, Zhou F. Glymphatic system dysfunction in recovered patients with mild COVID-19: A DTI-ALPS study. *Iscience* 2024, 27(1).
11. Theoharides TC, Cholevas C, Polyzoidis K, Politis A. Long-COVID syndrome-associated brain fog and chemofog: Luteolin to the rescue. *BioFactors*. 2021;47(2):232–41.
12. Pang Z, Tang A, He Y, Fan J, Yang Q, Tong Y, Fan H. Neurological complications caused by SARS-CoV-2. *Clin Microbiol Rev*. 2024;37(4):e00131–00124.
13. Krishnan K, Lin Y, Prewitt K-RM, Potter DA. Multidisciplinary approach to brain fog and related persisting symptoms post COVID-19. *J Health Service Psychol*. 2022;48(1):31–8.
14. Zhou Z, Zhao T, Sekendiz Z, Kritikos M, Fontana A, Clouston S, Luft B, Huang C. Impaired cerebrospinal fluid 18F-FEPPA clearance in long COVID suggests altered glymphatic system function. In: *Soc Nuclear Med*; 2024.
15. Langan MT, Smith DA, Verma G, Khegai O, Saju S, Rashid S, Ranti D, Markowitz M, Belani P, Jette N. Semi-automated segmentation and quantification of perivascular spaces at 7 Tesla in COVID-19. *Front Neurol*. 2022;13:846957.
16. Ren X, Liu S, Lian C, Li H, Li K, Li L, Zhao G. Dysfunction of the glymphatic system as a potential mechanism of perioperative neurocognitive disorders. *Front Aging Neurosci*. 2021;13:659457.
17. Kausel L, Figueroa-Vargas A, Zamorano F, Stecher X, Aspé-Sánchez M, Carvajal-Paredes P, Márquez-Rodríguez V, Martínez-Molina MP, Román C, Soto-Fernández P: patients recovering from COVID-19 who presented with anosmia during their acute episode have behavioral, functional, and structural brain alterations. *Sci Rep*. 2024;14(1):19049.
18. Faul F, Erdfelder E, Buchner A, Lang A-G. Statistical power analyses using G\* power 3.1: tests for correlation and regression analyses. *Behav Res Methods*. 2009;41(4):1149–60.
19. Yeh F-C, Zaydan IM, Suski VR, Lacomis D, Richardson RM, Maroon JC, Barrios-Martinez J. Differential tractography as a track-based biomarker for neuronal injury. *NeuroImage*. 2019;202:116131.
20. Frangi AF, Niessen WJ, Vincken KL, Viergever MA. Multiscale vessel enhancement filtering. In: *Medical Image Computing and Computer-Assisted Intervention—MICCAI'98: First International Conference Cambridge, MA, USA, October 11–13, 1998 Proceedings 1: 1998: Springer; 1998: 130–137.*
21. Choi Y, Nam Y, Choi Y, Kim J, Yang J, Ahn KJ, Kim Bs, Shin NY. MRI-visible dilated perivascular spaces in healthy young adults: A twin heritability study. *Hum Brain Mapp*. 2020;41(18):5313–24.
22. Patenaude B, Smith SM, Kennedy DN, Jenkinson M. A Bayesian model of shape and appearance for subcortical brain segmentation. *NeuroImage*. 2011;56(3):907–22.
23. Kim M, Hwang I, Park JH, Chung JW, Kim SM, Kim Jh, Choi KS. Comparative analysis of glymphatic system alterations in multiple sclerosis and neuromyelitis Optica spectrum disorder using MRI indices from diffusion tensor imaging. *Hum Brain Mapp*. 2024;45(5):e26680.
24. Bergamino M, Walsh RR, Stokes AM. Free-water diffusion tensor imaging improves the accuracy and sensitivity of white matter analysis in Alzheimer's disease. *Sci Rep*. 2021;11(1):6990.
25. Kim M, Choi KS, Hyun RC, Hwang I, Yun TJ, Kim SM, Kim J-h. Free-water diffusion tensor imaging detects occult periependymal abnormality in the AQP4-IgG-seropositive neuromyelitis Optica spectrum disorder. *Sci Rep*. 2022;12(1):512.
26. Smith SM, Jenkinson M, Johansen-Berg H, Rueckert D, Nichols TE, Mackay CE, Watkins KE, Ciccarelli O, Cader MZ, Matthews PM. Tract-based Spatial statistics: Voxelwise analysis of multi-subject diffusion data. *NeuroImage*. 2006;31(4):1487–505.
27. Smith SM, Nichols TE. Threshold-free cluster enhancement: addressing problems of smoothing, threshold dependence and localisation in cluster inference. *NeuroImage*. 2009;44(1):83–98.
28. Liu X, Barisano G, Shao X, Jann K, Ringman JM, Lu H, Arfanakis K, Caprihan A, DeCarli C, Gold BT. Cross-Vendor Test-Retest validation of diffusion tensor image analysis along the perivascular space (DTI-ALPS) for evaluating glymphatic system function. *Aging and Disease*; 2023.
29. Team J. JASP (Version 0.17)[Computer Software]. 2023. <https://jasp-stats.org>.
30. Friedman J, Hastie T, Tibshirani R. Sparse inverse covariance Estimation with the graphical Lasso. *Biostatistics*. 2008;9(3):432–41.
31. Bougakov D, Podell K, Goldberg E. Multiple neuroinvasive pathways in COVID-19. *Mol Neurobiol*. 2021;58(2):564–75.
32. Harapan BN, Yoo HJ. Neurological symptoms, manifestations, and complications associated with severe acute respiratory syndrome coronavirus 2 (SARS-CoV-2) and coronavirus disease 19 (COVID-19). *J Neurol*. 2021;268(9):3059–71.
33. Jessen NA, Munk ASF, Lundgaard I, Nedergaard M. The glymphatic system: a beginner's guide. *Neurochem Res*. 2015;40:2583–99.
34. Genç B, Buruk MS, Özçağlayan A, Kerim A. Alterations in the glymphatic system and presence of small vessel disease in hospitalized and Non-hospitalized COVID patients: A study of PSMD index and DTI-ALPS. *Academic Radiology*; 2025.
35. Rolls ET. The functions of the orbitofrontal cortex. *Brain Cogn*. 2004;55(1):11–29.
36. Zhou G, Lane G, Cooper SL, Kahnt T, Zelano C. Characterizing functional pathways of the human olfactory system. *Elife*. 2019;8:e47177.
37. Rolls ET, Critchley HD, Mason R, Wakeman EA. Orbitofrontal cortex neurons: role in olfactory and visual association learning. *J Neurophysiol*. 1996;75(5):1970–81.
38. Butowt R, von Bartheld CS. Anosmia in COVID-19: underlying mechanisms and assessment of an olfactory route to brain infection. *Neuroscientist*. 2021;27(6):582–603.
39. Royet J-P, Plailly J. Lateralization of olfactory processes. *Chem Senses*. 2004;29(8):731–45.
40. Wang J, Xia X, Zhang B, Ma X, Shi F, Wei Y, Li L, Meng X. Association of glymphatic system dysfunction with cognitive impairment in Temporal lobe epilepsy. *Front Aging Neurosci*. 2024;16:1459580.
41. Qin Y, Li X, Qiao Y, Zou H, Qian Y, Li X, Zhu Y, Huo W, Wang L, Zhang M. DTI-ALPS: an MR biomarker for motor dysfunction in patients with subacute ischemic stroke. *Front NeuroSci*. 2023;17:1132393.
42. Uchida Y, Kan H, Furukawa G, Onda K, Sakurai K, Takada K, Matsukawa N, Oishi K. Relationship between brain iron dynamics and blood-brain barrier function during childhood: a quantitative magnetic resonance imaging study. *Fluids Barriers CNS*. 2023;20(1):60.
43. Uchida Y, Kan H, Sakurai K, Horimoto Y, Hayashi E, Iida A, Okamura N, Oishi K, Matsukawa N. APOE E4 dose associates with increased brain iron and  $\beta$ -amyloid via blood-brain barrier dysfunction. *J Neurol Neurosurg Psychiatry*. 2022;93(7):772–8.
44. Uchida Y, Kan H, Sakurai K, Oishi K, Matsukawa N. Quantitative susceptibility mapping as an imaging biomarker for Alzheimer's disease: the expectations and limitations. *Front NeuroSci*. 2022;16:938092.
45. Uchida Y, Kan H, Sakurai K, Oishi K, Matsukawa N. Contributions of blood-brain barrier imaging to neurovascular unit pathophysiology of Alzheimer's disease and related dementias. *Front Aging Neurosci*. 2023;15:111448.

## Publisher's note

Springer Nature remains neutral with regard to jurisdictional claims in published maps and institutional affiliations.